Time domain analysis of a pultruded composite cooling tower under dynamic wind loads

João Paulo D. de S. Pereira[1], Eliane Maria L. Carvalho[1], Janine D. Vieira[1]

[1] Escola de Engenharia, Universidade Federal Fluminense (UFF)
Rua Passo da Pátria, 156, São Domingos, 24210-240, Niterói, RJ, Brazil
jp_dias@id.uff.br, elianemaria@id.uff.br, janinedv@id.uff.br

Abstract. Pultruded glass fiber reinforced polymer (pGFRP) profiles have been used in cooling tower frame structures for decades. Its advantageous properties such as high strength-to-mass ratio and corrosion resistance make it well-suited for the highly humid environment of cooling towers. On the other hand, pGFRP also has a relatively low modulus of elasticity, about 10% that of steel, which makes the structures more flexible. This results in low natural frequencies and brings the risk of resonance to dynamic loads such as wind fluctuation. The present study assesses the response of a pGFRP cooling tower under dynamic wind loads. A finite element (FE) model of the structure was developed to obtain its modal properties and assess the structure's dynamic response. A spectral representation method was implemented in Python to generate artificial wind fluctuation time series, which were input into the FE model to produce the fluctuating component of the wind drag force. The results show that, despite the flexibility, the structure satisfies the serviceability limit state and can be safely exposed to dynamic wind loads, benefitting from the material's favorable properties.

Keywords: Dynamics, Wind loads, Pultruded composite, Cooling towers.

1 Introduction

Fiber-reinforced polymers (FRP) are composite materials that consist of a polymeric matrix reinforced by fibers disposed in various architectures (e.g., rovings, mats, fabrics and veils). The combination leads to low density, high strength, good durability and low electrical conductivity, making the FRP competitive in relation to traditional materials such as concrete, steel and wood [1-4]. For this reason, interest in FRP solutions is growing in many areas, such as the aerospace, marine, oil and gas, automobile and construction industries [5, 6]. In civil and industrial construction, pultruded glass fiber reinforced polymer (pGFRP) profiles are most used as they provide a good balance between mechanical properties, durability and cost when compared to other types of fibers and FRP manufacturing processes [1, 7-10]. Due to their lightness, strength, durability and cost-effectiveness, pGFRP profiles have been used as secondary elements such as stairs, decks and handrails, and also as main structural parts in structures like footbridges, transmission towers and cooling towers [11, 12].

In this work, the response of a pGFRP cooling tower to fluctuating wind loads is assessed. Although the material has numerous advantageous properties, its modulus of elasticity is relatively low, about 10% that of steel. This results in more flexible structures, which tend to show large displacements and lower natural frequencies. According to the Brazilian standard for wind design NBR 6123 [13], if a structure shows natural frequencies below 1.0 Hz, the displacements caused by wind fluctuation might be amplified by resonance effects. As the analyzed structure meets this condition, a dynamic analysis in the time domain was carried out to evaluate its serviceability.

2 Description of the structure

The cooling tower consists of an 18 m x 18 m x 10.5 m frame made of pultruded glass fiber reinforced polymer (pGFRP) profiles with a total mass of 18.305 kg. Figure 1 shows the cross sections of the profiles used and a section of the structure with the location of components, whose masses are shown in Tab. 1.

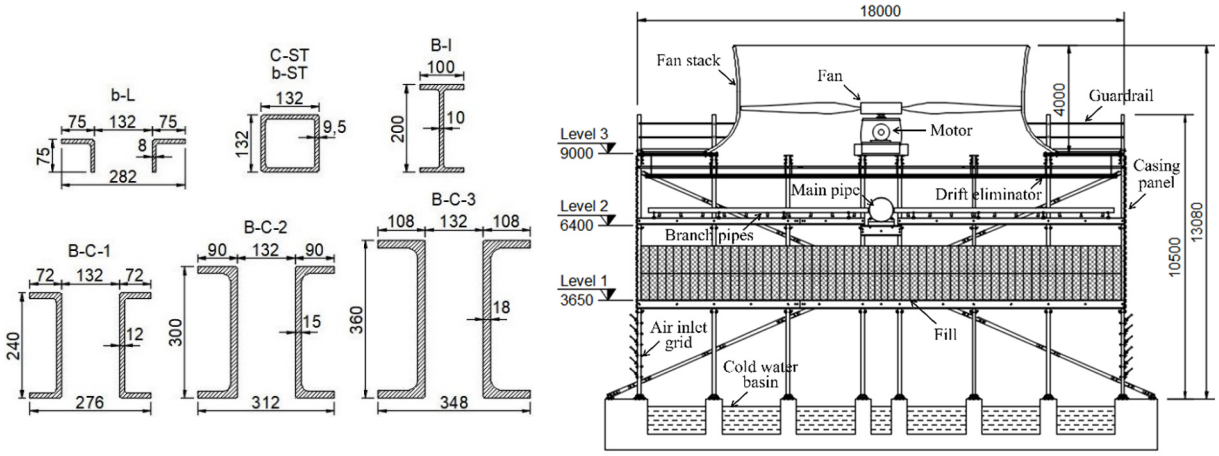

(a) (b)

Figure 1. (a) Cross section of the profiles and (b) sectional view of the structure (dimensions in mm).

Table 1. Component masses.

Mass source	Total mass (kg)	Location
Water	55,000	Levels 1 and 2
PVC fill	18,144	Level 1
GFRP main pipe	736	Level 2
PVC branch pipes	2,170	
Fan and motor	6,400	Level 3
pGFRP fan stack	4,800	
PVC drift eliminator	3,425	
pGFRP deck	7,740	
pGFRP guardrail	325	
pGFRP air inlet grid	1,235	Exterior columns
PVC casing panels	1,425	
Total (less water)	46,400	-

Profile shapes and mechanical properties of the pGFRP were obtained from Fiberline Composites [14] and the Brazilian pre-standard for the design of pultruded composite structures [15]. Table 2 shows the material properties, where ρ is the density, E_L the longitudinal modulus of elasticity, E_t the transversal modulus of elasticity, G the shear modulus, f_t the tensile strength, f_c the compression strength, f_v the shear strength, ξ the damping ratio, $\nu_{0^o,90^o}$ the major and $\nu_{90^o,0^o}$ the minor Poisson's ratio.

Table 2. Mechanical properties of pGFRP.

ρ (kg/m³)	E_L (GPa)	E_t (GPa)	G (GPa)	f_t (MPa)	f_c (MPa)	f_v (MPa)	ξ (%)	$\nu_{0^o,90^o}$	$\nu_{90^o,0^o}$
1,900	24.0	10.0	3.0	240	240	40	1.5	0.23	0.09

Back-to-back double channel beams were connected to square tube (ST) columns by through-bolts. I-beams were used to support the branch pipes and double angles were used for horizontal bracing (Fig. 2a). ST bracings

were added to the outer columns in an X-shape, and column bases were bolted to the foundation with steel angles (Fig. 2b).

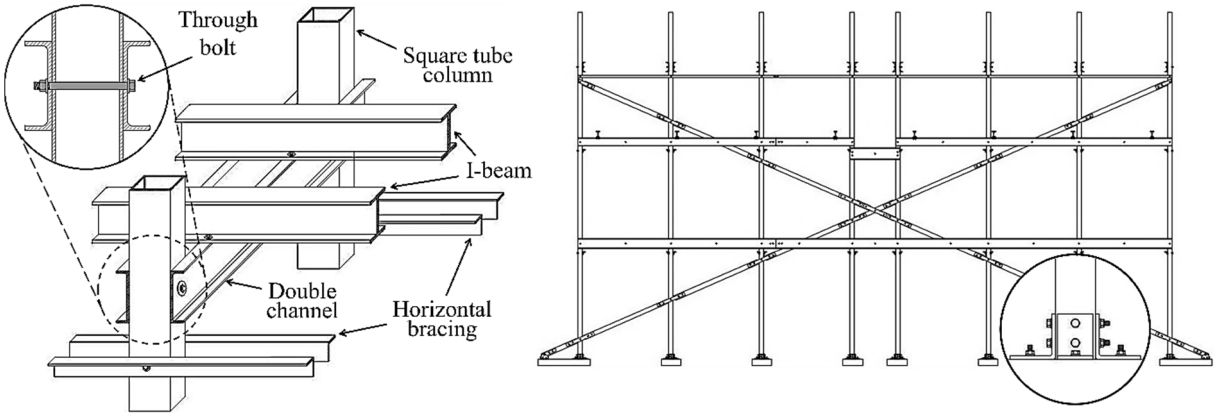

(a) (b)

Figure 2. (a) Beams, columns and horizontal bracing; (b) vertical bracing and column base support.

3 Analysis methodology

A 3D model of the structure was developed in SAP2000 v.14.0.0 [16], a commercial software based on the finite element (FE) method, to obtain the modal properties of the structure. A Python code was written to generate the artificial time series of fluctuating wind speed, which were input to the FE model as a time-dependent load to analyze the structure's dynamic response.

3.1 FE modeling

Columns, beams, bracing members and linear components such as the air inlet grid and the guardrail were modeled using bar elements, as shown in Fig. 3a. Shell elements were used for the deck, fan stack and casing panels. Gravity loads were applied to the beams and deck, and horizontal wind loads were applied to wind obstructing components (Fig. 3b). Link elements with released rotational stiffnesses were used to model the eccentricity of beams and the pin behavior of bolted joints (Fig. 4). The supports were modeled as pinned, and the masses of non-structural components were added to the model to take into account their contribution to the dynamic response of the structure.

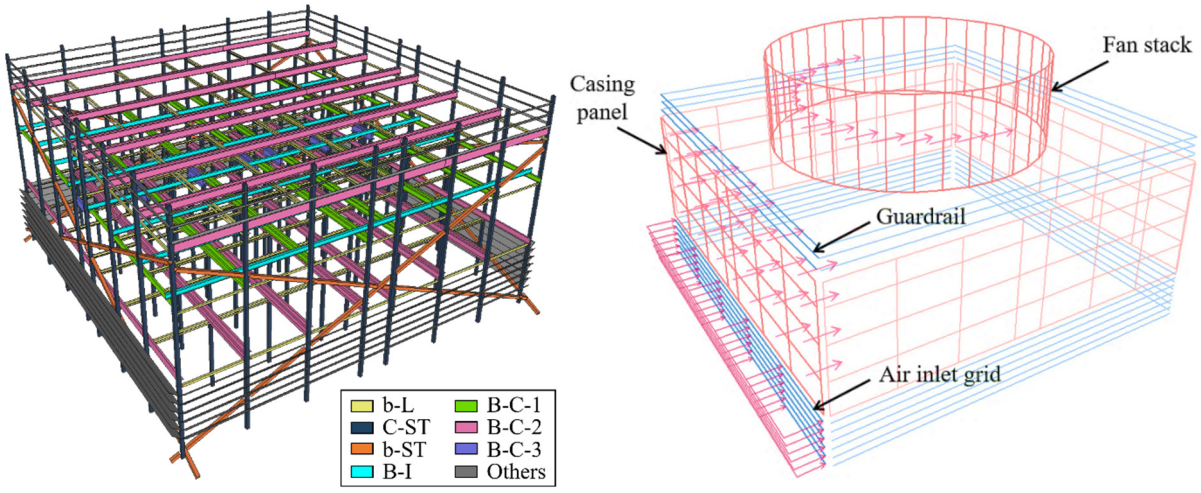

(a) (b)

Figure 3. (a) Solid view of bar elements and (b) wind load application.

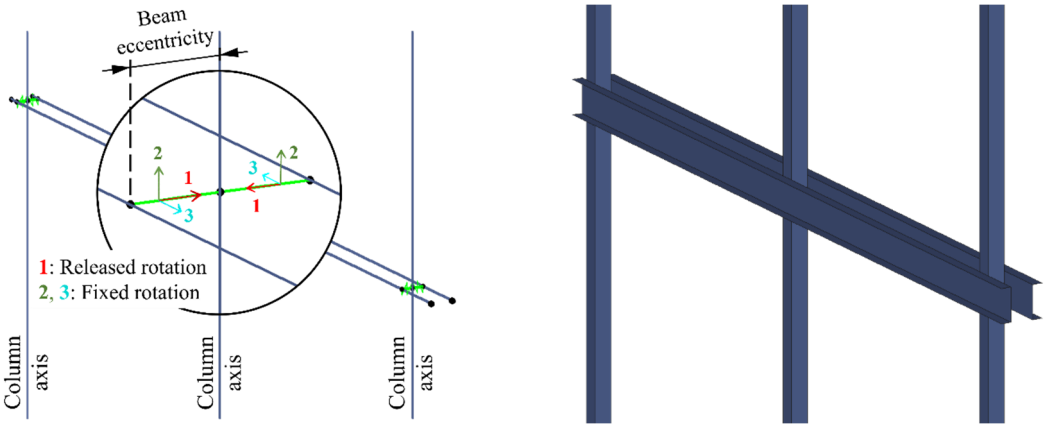

(a) (b)

Figure 4. (a) Wireframe and (b) solid view of beam-column joints.

3.2 Modal analysis

The modal analysis was carried out using the eigenvector method, and the criteria for the number of vibration modes was to capture at least 80% of mass participation (MP) in each horizontal direction. With 200 modes, MP of 95.3% and 84.2% were found in X and Y directions, respectively. Table 3 shows the natural frequency f_n and MP of the most relevant modes, whose mode shapes are shown in Fig. 5.

Table 3. Most relevant vibration modes in each direction.

Mode no.	Direction	f_n (Hz)	MP (%)
1	Y	0.70	38.0
2	X	0.93	63.5

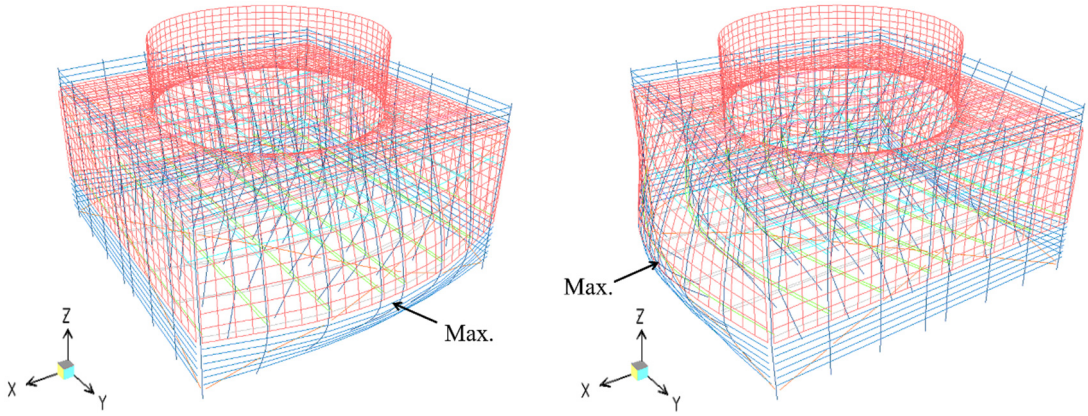

(a) (b)

Figure 5. Mode shapes of (a) the 1st and (b) the 2nd vibration modes.

3.3 Wind load simulation

The wind drag force F(z, t), function of height z and time t, is calculated by the following equation:

$$F(z, t) = \frac{\rho_{air}\, C_a\, A\, U^2(z, t)}{2}, \tag{1}$$

where ρ_{air} = 1.226 kg/m³, C_a = 0.95 and A are the air density, drag coefficient and wind obstruction area, respectively. The longitudinal wind speed U(z, t) is given by the sum of an average component $\bar{U}(z)$ and a fluctuating component u(t). It is worth noting that the square of U(z, t) produces a non-linear term $u^2(t)$. However,

since the standard deviation of the fluctuation, σ, was found to be around 20% of the mean wind speed, the linear term is dominant [17] and the quadratic term was neglected. Equation 1 can be rewritten as:

$$F(z,t) = \frac{\rho_{air}\, C_a\, A\, [\bar{U}^2(z) + 2\,\bar{U}(z)\,u(t)]}{2}. \tag{2}$$

The design value of $\bar{U}(z)$ was calculated by:

$$\bar{U}(z) = 0.86\, U_0 \left(\frac{z}{10}\right)^{0.12}, \tag{3}$$

where $U_0 = 32.5$ m/s is the basic wind speed at the city of Rio de Janeiro [13].

The fluctuation u(t) was simulated using the spectral representation method presented by Shinozuka and Jan [18]. A power spectral density (PSD) function based on wind speed records, S(f), is discretized in k = 1, 2… N intervals and the fluctuation is calculated as a series of weighted amplitude cosine waves:

$$u(t) = \sum_{k=1}^{N} \sqrt{2\, S(f_k)\, \Delta f}\, \cos(2\pi\, f_k\, t + \theta_k), \tag{4}$$

where θ_k is a random phase angle with uniform distribution from 0 to 2π and Δf is the length of each interval. Based on Zang et al. [19], the power spectrum proposed by Davenport [20] was used in this work. It is given by:

$$\frac{f\, S(f)}{u_*^2} = \frac{4\, [1200\, f/\bar{U}(10)]^2}{\{1 + [1200\, f/\bar{U}(10)]^2\}^{4/3}}, \tag{5}$$

where f is the frequency in Hz. The friction velocity u_* is given by:

$$u_* = \frac{0.4\, \bar{U}_{600}(10)}{\ln(10/z_0)}, \tag{6}$$

where $z_0 = 1.0$ m is the terrain roughness length for a well-developed industrial site and $\bar{U}_{600}(z)$ is the average wind speed for an analysis interval T = 600 s, calculated according to [13]:

$$\bar{U}_{600}(z) = 0.49\, U_0 \left(\frac{z}{10}\right)^{0.23}. \tag{7}$$

A fast Fourier transform (FFT) algorithm was applied to the fluctuation time series to validate the simulation. The number of samples $N = 2^{11} = 2{,}048$ was used, resulting in a time step $\Delta t = T/N = 0.29$ s, a sampling rate $f_s = N/T = 3.41$ Hz and a frequency step $\Delta f = f_s/N = 1.67$ mHz. The PSD of the simulation was calculated by:

$$S_k = \frac{1}{N\, f_s}\left(\sum_{n=0}^{N-1} u_n\, e^{\frac{-i2\pi kn}{N}}\right)^2, \tag{8}$$

where n is the time sample index ($t_n = t_{n-1} + \Delta t$) and k the frequency index ($f_k = f_{k-1} + \Delta f$). Figure 6 shows a random time signal of u(t) and the comparison between the simulated PSD and the target spectrum by Davenport (Eq. 5).

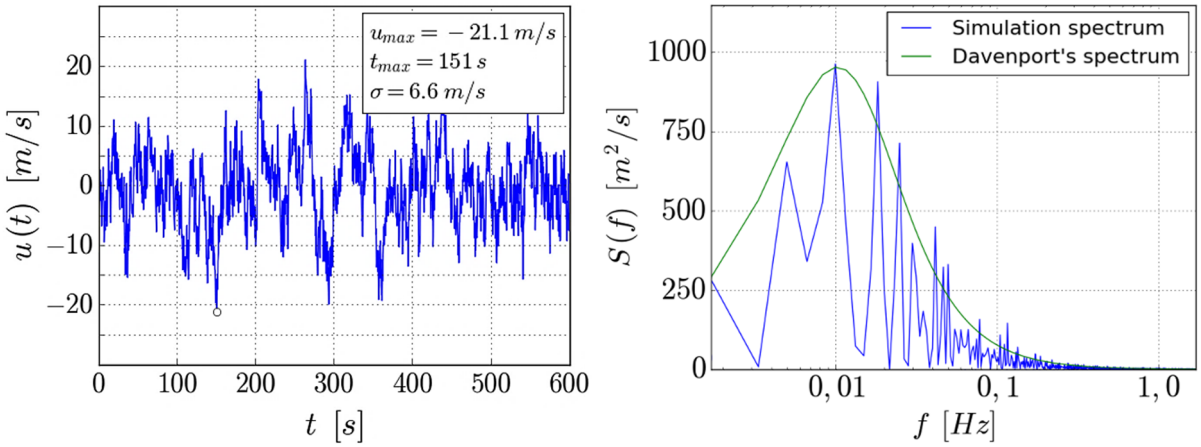

(a) (b)

Figure 6. (a) Time signal of wind fluctuation; (b) simulation and Davenport's PSD.

The wind fluctuation was considered perfectly correlated at all the points of the structure due to its dimensions being shorter than the transversal turbulence length scales, L_u^y = 20.7 m (horizontal) and L_u^z = 31.0 m (vertical), which were calculated by [21, 22]:

$$L_u^y = L_u^x/3\,, \tag{9}$$

$$L_u^z = L_u^x/2\,, \tag{10}$$

$$L_u^x = 280\left(\frac{z}{1000\, z_0^{0.18}}\right)^{0.35}, \tag{11}$$

where L_u^x is the longitudinal turbulence length scale.

A total of 20 simulations were run and the time series of u(t) were input into SAP2000 to generate the time-dependent component of F(z, t) shown in Eq. 2.

4 Results and discussion

Verifications were carried out with load combinations from NBR 8681 [23]. A factor of 0.3 was used for wind load in serviceability limit state (SLS). Table 4 shows the verification of lateral displacement SLS, where δ_{av} and δ_{din} are the average and dynamic components of the displacement δ, statistically calculated from 20 simulations. Given the height at the top of the columns H = 10.5 m, the limit displacement was set as δ_{lim} = H/400 = 26.3 mm. Figure 7 shows spectral displacement and acceleration responses of the structure in the Y direction.

Table 4. Verification of lateral displacement SLS.

Direction	δ_{av} (mm)	δ_{din} (mm)	δ (mm)	δ/δ_{lim} (%)
X	4.8	12.0 ± 1.4	16.8 ± 1.4	64 ± 5 ✓
Y	5.7	14.7 ± 1.3	20.4 ± 1.3	78 ± 5 ✓

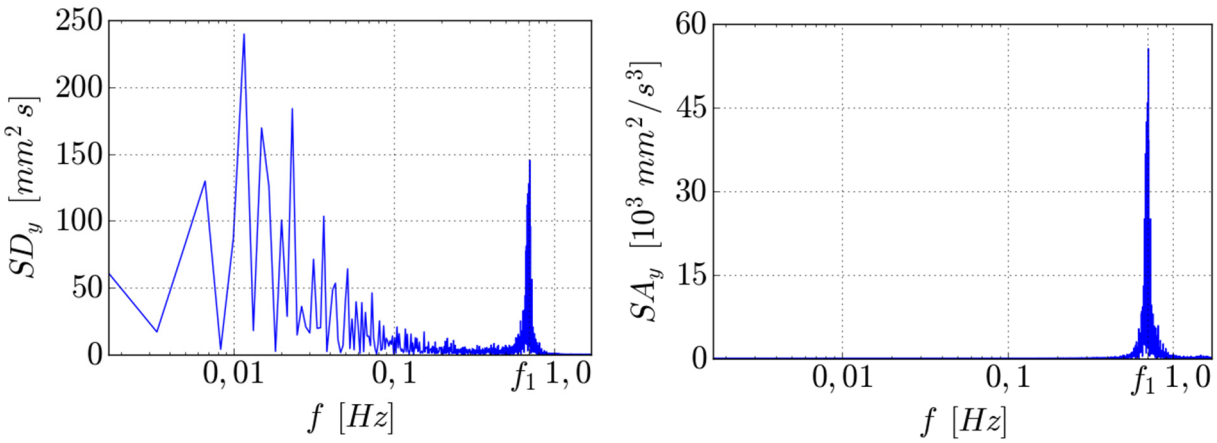

(a) (b)

Figure 7. PSD of (a) displacement and (b) acceleration responses in the Y direction.

It can be seen in Fig. 7 that the lower frequency harmonics of wind fluctuation induce a quasi-static response, accounting for most of the structure's displacement and having no correspondence in the acceleration response. At the natural frequency f_1, a peak is observed for both the displacement and acceleration responses, corresponding to the resonant response of the structure. These observations can be attributed to low frequencies (up to 0.2 Hz) having most of the energy in the wind speed power spectrum (see Fig. 6b), while the structure's resonant frequencies lie on a low energy range (closer to 1.0 Hz).

5 Conclusions

The dynamic analysis of the structure has proven that, although the first natural frequencies lie below 1.0 Hz, the displacements induced by wind fluctuation satisfy the serviceability requirements. The response of the structure was mainly quasi-static due to the low-frequency harmonics, with a small portion induced by resonant frequencies. This means that, although pGFRP has a relatively low modulus of elasticity, a structure like the one shown can make good use of the material's advantageous properties and be safely exposed to wind loads.

Acknowledgements. The authors would like to acknowledge the financial support from the Rio de Janeiro State Research Support Foundation (FAPERJ).

Authorship statement. The authors hereby confirm that they are the sole liable persons responsible for the authorship of this work, and that all material that has been herein included as part of the present paper is either the property (and authorship) of the authors, or has the permission of the owners to be included here.

References

[1] D. K. Rajak, P. H. Wagh and E. Limul, "Manufacturing technologies of carbon/glass fiber-reinforced polymer composites and their properties: A review". *Polymers*, vol. 13, n. 21, pp. 1-42, 2021.
[2] M. R. M. Asyraf, M. R. Ishak, S. M. Sapuan and N. Yidris, "Comparison of static and long-term creep behaviors between Balau wood and glass fiber reinforced polymer composite for cross-arm application". *Fibers and Polymers*, vol. 22, pp. 793-803, 2021.
[3] E. Madenci and A. S. Ecemiş, "Comparative study on 2D pultruded GFRP composite and conventional frame structures using ETABS". In: A. Asrlaner, D. Tekin, S. A. Güven, S. Emeş and T. Elbir (eds.), *4th International Conference on Advanced Engineering Technologies (ICADET 22)*, n. 34, pp. 274-278. Bayburt University Publications, 2022.
[4] L. Mincigrucci, M. Civera, E. Lenticchia, R. Ceravolo, M. Rosano and S. Russo, "Comparative structural analysis of GFRP reinforced concrete and steel frames under seismic loads". *Materials*, vol. 16, n. 14, pp. 1-17, 2023.
[5] J. R. Correia, "Fibre-reinforced polymer (FRP) composites". In: M. C. Gonçalves and F. Margarido (eds.), *Materials for construction and civil engineering*, pp. 501-556. Springer, 2015.
[6] A. Vedernikov, A. Safonov, F. Tucci, P. Carlone and I. Akhatov, "Pultruded materials and structures: A review". *Journal of Composite Materials*, vol. 56, n. 26, pp. 1-37, 2020.
[7] I. S. Abbood, S. A. Odaa, K. F. Hasan and M. A. Jasim, "Properties evaluation of fiber reinforced polymers and their constituent materials used in structures – A review". *Materials Today: Proceedings*, vol. 43, pt. 2, pp. 1003-1008, 2021.
[8] B. L. Ennis, S. Das and R. E. Norris, "Economic competitiveness of pultruded fiber composites for wind turbine applications". *Composites Part B: Engineering*, vol. 265, pp. 1-13, 2023.
[9] A. M. Fairuz, S. M. Sapuan, E. S. Zainudin and C. N. A. Jaafar, "Polymer composite manufacturing using a pultrusion process: A review". *American Journal of Applied Sciences*, vol. 11, n. 10, pp. 1798-1810, 2014.
[10] M. Volk, O. Yuksel, I. Baran, J. H. Hattel, J. Spangenberg and M. Sandberg, "Cost-efficient, automated, and sustainable composite profile manufacture: A review of the state of the art, innovations, and future of pultrusion technologies". *Composites Part B*, vol. 246, pp. 1-14, 2022.
[11] J. Qureshi, "A review of fibre reinforced polymer structures". *Fibers*, vol. 10, n. 3, pp. 1-29, 2022.
[12] K. P. Mortensen and R. W. Petterson, "Fiberglass reinforced polyester in cooling towers – Structural application". In: *Cooling Technology Institute Annual Conference 2013*, pp. 1-12. Cooling Technology Institute, 2013.
[13] Associação Brasileira de Normas Técnicas. *NBR 6123: Forças devidas ao vento em edificações*. ABNT, 2023.
[14] Fiberline Composites A/S. *Fiberline design manual*. Kolding, 2003.
[15] Associação Brasileira de Normas Técnicas. *Projeto de estruturas de perfis pultrudados de PRFV [Pre-standard]*. ABNT/CEE-40, 2024.
[16] Computers & Structures, Inc. (CSI). *SAP2000 v.14.0.0*. Walnut Creek, 2009.
[17] A. H. Monahan, "The temporal autocorrelation structure of sea surface winds". *Journal of Climate*, vol. 25, pp. 6684-6700, 2012.
[18] Shinozuka and Jan, "Digital simulation of random processes and its applications". *Journal of Sound and Vibration*, vol. 25, n. 1, pp. 111-128, 1972.
[19] C. C. Zang, J. K. Yuan, J. Sment, A. C. Moya, C. K. Ho and Z. F. Wang, "Numerical simulation of wind loads and wind induced dynamic response of heliostats". *Energy Procedia*, vol. 49, pp. 1582-1591, 2014.
[20] A. G. Davenport, "The spectrum of horizontal gustiness near the ground in high winds". *Quarterly Journal of the Royal Meteorological Society*, vol. 87, n. 372, pp. 194-211, 1961.
[21] E. Simiu and D. Yeo. *Wind effects on structures: Modern structural design for wind*. John Wiley & Sons, 2019.
[22] D. Romanic, D. Parvu and H. Hangan, "Fluctuating wind generator: Theoretical concept and model". In: *1000 Islands Fluid Mechanics Meeting 2016* (TIM 2016).
[23] Associação Brasileira de Normas Técnicas. *NBR 8681: Ações e segurança nas estruturas – Procedimento*. ABNT, 2003.